minerals

Article

Burial and Thermal History Modeling of the Paleozoic–Mesozoic Basement in the Northern Margin of the Western Outer Carpathians (Case Study from Pilzno-40 Well, Southern Poland)

Dariusz Botor

Faculty of Geology, Geophysics and Environmental Protection, AGH University of Science and Technology, 30-059 Kraków, Poland; botor@agh.edu.pl

Abstract: Hydrocarbon exploration under thrust belts is a challenging frontier globally. In this work, 1-D thermal maturity modeling of the Paleozoic–Mesozoic basement in the northern margin of the Western Outer Carpathians was carried out to better explain the thermal history of source rocks that influenced hydrocarbon generation. The combination of Variscan burial and post-Variscan heating due to elevated heat flow may have caused significant heating in the Paleozoic basement in the pre-Middle Jurassic period. However, the most likely combined effect of Permian-Triassic burial and Late Triassic–Early Jurassic increase of heat flow caused the reaching of maximum paleotemperature. The main phase of hydrocarbon generation in Paleozoic source rocks developed in pre-Middle Jurassic times. Therefore, generated hydrocarbons from Ordovician and Silurian source rocks were lost before reservoirs and traps were formed in the Late Mesozoic. The Miocene thermal overprint due to the Carpathian overthrust probably did not significantly change the thermal maturity of organic matter in the Paleozoic–Mesozoic strata. Thus, it can be concluded that petroleum accumulations in the Late Jurassic and Cenomanian reservoirs of the foreland were charged later, mainly by source rocks occurring within the thrustbelt, i.e., Oligocene Menilite Shales. Finally, this work shows that comprehensive mineralogical and geochemical studies are an indispensable prerequisite of any petroleum system modelling because their results could influence petroleum exploration of new oil and gas fields.

Keywords: maturity modeling; Carpathians; Carpathians Foredeep; Paleozoic–Mesozoic basement; petroleum origin; hydrocarbon generation

check for updates

Citation: Botor, D. Burial and Thermal History Modeling of the Paleozoic–Mesozoic Basement in the Northern Margin of the Western Outer Carpathians (Case Study from Pilzno-40 Well, Southern Poland). *Minerals* **2021**, *11*, 733. https://doi.org/10.3390/min11070733

Academic Editors: Stavros Kalaitzidis, Jan Golonka and Petr Skupien

Received: 16 April 2021
Accepted: 2 July 2021
Published: 6 July 2021

1. Introduction

Hydrocarbon exploration under thrust belts is a challenging frontier, both in the Carpathians and, in general, globally, e.g., [1,2]. The most intriguing feature of the occurrence of oil and gas fields around the Carpathians and its foredeep is their existence not only within the orogen, but also within a relatively short distance from the orogenic front [3]. This highlight can be noticed along the entire Carpathian arch from Czechia across Poland, and Ukraine to Romania. The Carpathian Foredeep is one of the most prolific basins in Poland, accounting for more than 100 discoveries of dry methane gas in Miocene strata. The total reserves of these fields comprise 138 billion cubic meters. To date, 13 natural gas fields and 10 oil fields have been discovered in the Mesozoic and Paleozoic of the Carpathian Foredeep and the sub-Carpathian basement. These fields have combined reserves of 7.5 billion cubic meters of gas and 4.7 million tons of oil [4].

Thermal and maturity modeling (basin modeling) is used as a tool for the charge element assessment when risking a play or a prospect. One-dimensional (1-D) maturity modeling of the potential source rock intervals of the modeled section is widely applied to reconstruct the burial and thermal history of sedimentary basins, e.g., [5–8]. The mean random vitrinite reflectance (VR) measurements are now widely used to establish the thermal maturity level of organic matter in source rocks, e.g., [9,10]. One of the main outputs of this 1-D basin modeling is the establishment of the timing of hydrocarbon generation. However, it is difficult to precisely determine this timing because several options relating to the thermal history, which govern hydrocarbon generation, exist in many cases [11]. To limit the number of possible hypotheses of thermal evolution, it is necessary to apply independent mineral and geochemical methods, including isotope dating methods, which provide insights into the interpretation of the thermal history. The aim of the current study is to present new models of burial and thermal evolution of the Paleozoic–Mesozoic basement in the frontal Carpathian orogenic wedge. Recently published works show that the Carpathian tectonic load in the frontal orogenic zone is not as significant as previously assumed, e.g., [12]. Therefore, explaining pre-orogenic evolution is crucial for establishing effective source rocks for hydrocarbon charge, particularly in Mesozoic reservoirs.

2. Geological Setting

2.1. Carpathians

The Carpathians are subdivided into two main regions: Outer- and Intra-Carpathians (Figure 1). The Intra-Carpathian region is composed of two major continental blocks: (a) Alcapa—the Eastern Alpine–Western Carpathian–Northern Pannonian; and (b) Tisza—the Southern Pannonian–Eastern Carpathian [12,13]. The Outer Carpathians are an external part of an elongated fold-and-thrust belt, e.g., [13–16]. The northern part of this belt, which belongs to the Western Outer Carpathians, occurs within Poland. The origin of the Carpathians is related to the convergence and collision of the European and African plates, which formed part of the European Alpine chain [16–18]. The collision of these two plates was diachronous; it began in the Middle Cretaceous and has probably continued to the present. Indentation of the continental fragment called the Alcapa block [13] was the main reason for the formation of the Western Outer Carpathians [14,19]. During the Cenozoic. the Western Outer Carpathians was formed as an accretionary prism related to the approximately southward subduction of the European plate. The Polish part of the Western Outer Carpathians is a north-verging fold-and-thrust belt composed largely of Lower Cretaceous to Miocene flysch sediments, arranged in a stacked complex of several nappes (from top to bottom, the major ones are: Magura, Dukla and Fore-Magura, Silesian, Sub-Silesian, and Skole nappes (Figures 1 and 2) [15,16,20].

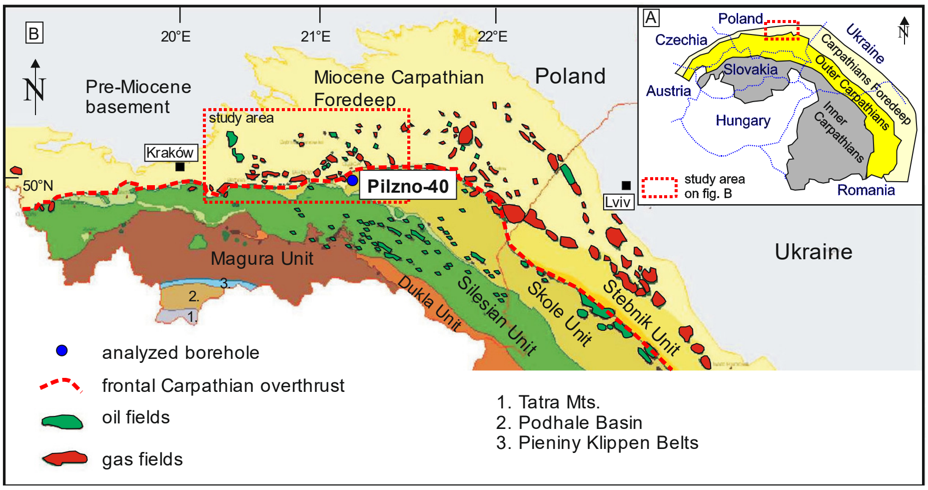

Figure 1. Location of the study area including oil and gas fields overlaid on simplified geology (**A**,**B**); modified from [3,4,14].

The tectonic evolution of the Polish Outer Carpathians is subdivided into two successive shortening events: (1) NNW-(N)-directed and (2) NE-(NNE)-directed [21–24]. During the first event, the folding and thrusting started in the most inner, southern nappe (Magura) and propagated to the north. During the next event, the previous thrust faults, in addition to folds, were overprinted and refolded. The first shortening event occurred from the Eocene to Early Miocene period [23,25]. The second shortening event started in the Early/Middle Miocene [23], but lasted until the early Late Miocene period ([20,24] and references therein). Vitrinite reflectance (VR) values of the flysch strata range significantly, indicating a wide spectrum of thermal maturity. Generally, VR values point to immature to mature stages (oil windows) and, locally, to gas windows in different units of the Outer Carpathians [26–29].

2.2. Carpathian Foredeep

Generally, the Polish part of the Carpathian Foredeep developed during the Early and Middle Miocene as a peripheral flexural foreland basin in front of the thrusting Carpathians [3,30–32]. This basin can be subdivided into an inner and an outer part. The inner foredeep is located south of the Carpathian frontal thrust and contains up to 1500 m of Lower to Middle Miocene (mainly terrestrial) deposits that are overridden by thrust sheets. The outer foredeep is filled by Middle Miocene (Badenian and Sarmatian) shallow-marine deposits, which range in thickness from a few hundred metres in its northern, marginal parts, to as much as 3.5 km in its SE parts adjacent to the Carpathian thrust front [3,30–32].

The different parts of the Carpathian thrust front have been interpreted in terms of wedge tectonics [33,34]. The major collisional deformations of the study area took place in the Miocene; however, these processes started in the Oligocene or Eocene [15,25]. The youngest foredeep sediments are of Sarmatian age, indicating that the latest thrust movements of the frontal Carpathian orogenic in the study area occurred ca. 10 Ma [34], which allows maximum burial age in the study area to be established. Apatite fission track analyses and helium dating indicate that the foredeep Miocene succession in the Pilzno-40 area has not been buried deeper than 1.5 to 2 km [34], assuming a paleogeothermal gradient of the order of 25 to 29 °C/km [35,36]. This interpretation is consistent with reconstruction based on the seismic data [34], and the low thermal maturity of organic matter in the Miocene strata of the Carpathian Foredeep, which is in the range of 0.3 to 0.6%VR [37,38]. In the Czech area of the Carpathian Foredeep, even at a depth of 4300 m, thermal maturity is 0.58%VR in the Miocene sediments [39].

2.3. Basement of Carpathian Foredeep

The Carpathian Foredeep basement includes rocks from the Proterozoic to the Cretaceous. The depth to the top surface of the platform basement varies from several hundred meters to ca. 3500 m. The oldest structural element of the crystalline basement belongs to the Małopolska Block and has the Kraków–Lubliniec Fault Zone as its western margin. The northern margin of this block is commonly indicated along the Holy Cross Fault Zone ([40], and references therein). The deposition of the sedimentary cover of the Małopolska Block is divided into three structural stages: Caledonian, Variscan, and Alpine [40,41]. In the study area, the Paleozoic and Mesozoic sedimentary succession is characterized by numerous erosional gaps, and consists of Ordovician, Silurian, Devonian, Carboniferous, Permian, Triassic, Jurassic, and Cretaceous strata that are buried beneath the Miocene infill of the Carpathian Foredeep Basin and, partly, by the Carpathian thrust sheets [40–42].

In the study area, in the western part of the Małopolska block, the Caledonian stage is composed of Ordovician and Silurian strata, which rest directly above the Ediacaran anchimetamorphic complex [40]. The Middle to Late Ordovician strata includes carbonate and clastic complex of a changeable thickness, up to a few hundred meters, and the Lower Silurian, dark-colored, fine-grained claystone and mudstone sequence, up to 200 m thick [42]. Intensive post-Silurian erosion occurred in the study area; therefore, the occurrence of Lower Paleozoic strata is highly limited [40]. The Variscan structural stage is formed by the Lower Devonian, and/or the Middle Devonian–Lower Carboniferous carbonate and Lower Carboniferous clastic complexes [40,41,43]. The terrigenous deposits of the Lower Devonian are up to 200 m thick. The carbonates of the Middle and Upper Devonian range from 300 m in the east [44] to ca. 1000 m in the western part of the study region [45]. Overlying carbonate and clastic facies of the late Tournaisian–early Namurian (Carboniferous) [41] have thicknesses ranging from 80 m to 600 m, and from a few meters to 500 m, respectively. However, in some areas, Variscan erosion that developed in the Late Carboniferous and Permian removed sedimentary succession until the Lower Silurian, as seen in the examined Pilzno-40 well. In the study area, the thermal maturity of Paleozoic strata ranged from ca. 0.6 to 1.0%VR but locally reached up to 1.6%VR, indicating that Variscan erosion was very high considering the present-day depth of these rocks [46–48].

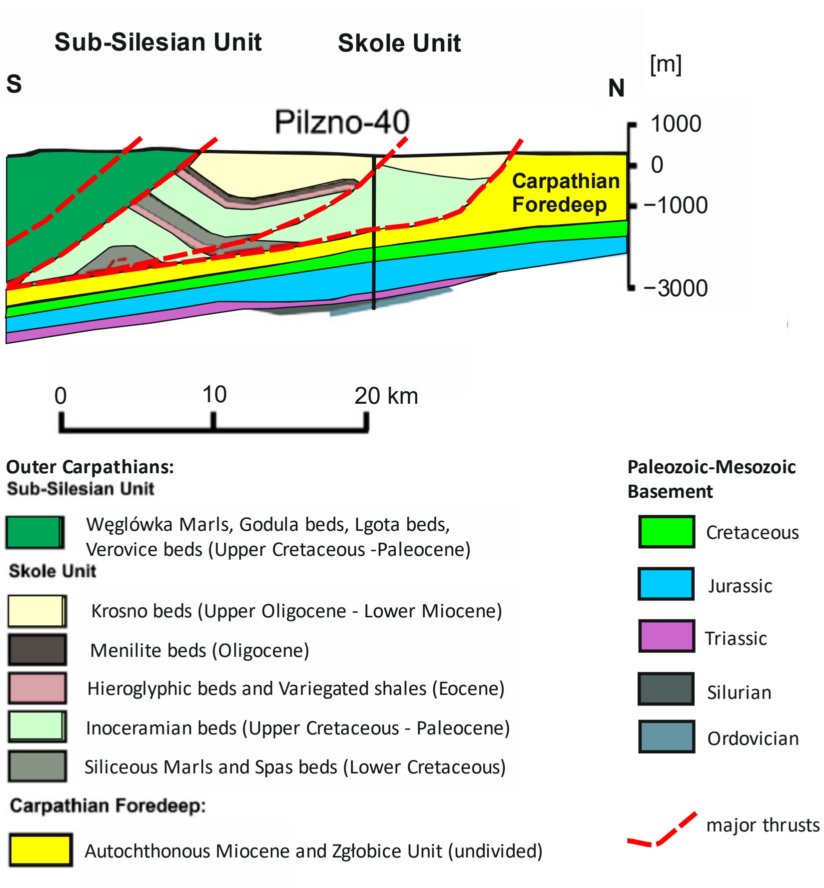

Figure 2. Simplified cross-section perpendicular to Carpathian orogenic front modified after [3,30,32,38].

The Permian–Mesozoic sedimentary cover is represented by the undivided Permian–Triassic complex, and the Middle Jurassic to Upper Cretaceous complexes. Their present areal extent and mutual relationships were determined by multistage processes of uplift [41], which led to significant erosion of the Mesozoic cover and reduction in the areal distribution of particular complexes, particularly the Permian–Triassic complex [41,49]. This had a significant influence on the burial history of the study area, where Lower Triassic terrigenous sediments lay directly on Lower Silurian shales, and are covered by the most widely distributed Jurassic to Cretaceous strata. Middle Jurassic (Upper Bajocian–Callovian) sediments are represented mainly by sandstone and siltstones [42]. The thickness of the Middle Jurassic deposits usually varies from 0 to even ca. 100 m in few wells. Above, there is a thick complex of the Upper Jurassic–Lower Cretaceous (Oxfordian to Hauterivian) carbonates. At present, due to erosional cut, the state of preservation of these strata is diversified: from 300 m in the vicinity of Kraków to ca. 1000 m in the Rzeszów area [49–53]. The Upper Cretaceous sediments are separated from the underlying strata by an erosional unconformity corresponding to the Austrian phase of regional deformation during Aptian and Albian times [41]. The Upper Cretaceous strata include up to ca. 120-m-thick Cenomanian sandstones [42], which are the main reservoir rocks apart from Upper Jurassic carbonates. These strata are overlaid by Turonian–Maastrichtian marly limestones and marls that are regarded to be sealing rocks (together with Miocene claystones/mudstones). The development and thickness of Mesozoic strata was determined by several Mesozoic and Cenozoic erosional phases, and polyphase Cretaceous/Paleogene block tectonics [42]. Therefore, the Mesozoic organic matter was found to be immature or at early maturity with VR values up to 0.78% [52,53]. Traps in Mesozoic accumulations were likely formed during the Cretaceous/Paleogene tectonic phase; however, the most common traps are the combination of structural and stratigraphic types. Traps are related to the sub-Miocene unconformities, and less related to the sub-Cretaceous unconformities. The pinching-out stratigraphic traps are known from the Cenomanian sandstones [1–4,15].

2.4. Source Rocks

In the Outer Carpathians, the Oligocene Menilite Shales are excellent effective source rocks for the conventional hydrocarbon reservoirs and provide perspective for the unconventional reservoirs. The thicknesses of the Menilite Shales are often elevated due to repetition during overthrusting and reach up to 1800 m in the Boryslav-Pokuttya and Skyba Units, up to 500 m in the Skole Unit, and up to about 100 m in the Silesian Unit [3,15,54]. The Menilite Shales are organic-rich and contain varying mixtures of oil-prone type-II, type-IIS, and admixture type-III kerogen. The total organic carbon (TOC) content of the shales frequently exceeds 20 wt.% and averages ca. 5 to 10 wt.%. The hydrogen index (HI) values range between 300 and 800 mg HC/g TOC [55–61]. The thermal maturity of Menilite Shales' organic matter is variable across the Outer Carpathians [55–61]. In the study area, the highest maturity is observed in the Dukla Unit, and corresponds to the peak and final stage of the oil window, whereas the organic matter dispersed in the Silesian Unit is usually immature. However, results of petroleum generation modelling by Matyasik and Dziadzio [54] suggest that the Menilite Shales in the deepest synclines of the Silesian Unit reaches sufficient maturity for generation of thermogenic hydrocarbons. In contrast, the Lower Cretaceous to Eocene strata in the Outer Carpathians have variable hydrocarbon potential, with low TOC values (below 1.0 wt.%). Type-III kerogen dominates in these beds with local admixtures of type-II kerogen. Thermal maturity comprises the whole range of the oil window. Type-III kerogen in the Upper Oligocene–Lower Miocene Krosno Beds is immature and their hydrocarbon potential is low [58]. In the Miocene strata of the Carpathian Foredeep, microbial gases are widely known and are the dominant natural gases in reservoirs. Their sources are an organic-rich interval within the Miocene succession that contains type-III kerogen [38].

In the pre-Miocene basement, possible source rocks are horizons occurring within the Ordovician, Silurian, Middle-Upper Devonian, and Lower Carboniferous [38,46,47]. Due to their immature to very low mature character, Mesozoic rocks cannot be proven to be source rocks, despite the fact that some of the these, such as Jurassic rocks, contain significant amounts of organic carbon [38,52].

Based on geochemical data, the initial TOC in the source rocks of the Paleozoic basement of the Carpathian Foredeep was calculated to be ca. 1.2 to 3.5% for siliciclastic Ordovician and Silurian rocks, 1.2% for carbonates of Middle-Upper Devonian, and 1.3% for siliciclastic of Lower Carboniferous [47]. The kerogen type is mainly type-II oil-prone low-sulfur in Ordovician and Silurian rocks, whereas it is type II with an admixture of type III in Middle-Upper Devonian and Lower Carboniferous rocks. The thickness of these source rocks is ca. 40 to 50 m for the Silurian, up to 100 to 150 m for siliciclastic of the Lower Carboniferous and Ordovician, and 200 to 300 m of the Middle-Upper Devonian [38,46,47]. All Paleozoic source rocks show a thermal maturity that allows thermogenic hydrocarbon generation [38,46,47].

Geochemical data showed that many oil and gas fields (e.g., Grobla, Rajsko, Rylowa, and Wierzchosławice) contain similar hydrocarbons in the Upper Jurassic carbonate and

Cenomanian sandstone reservoirs. These hydrocarbons were generated during thermogenic processes and probably migrated through the fault zones from source rocks. The Lower Carboniferous and Middle-Upper Devonian strata, and/or the Ordovician to Silurian rocks [38,47,62] or the Menilite Shales [55,56,63], are regarded to be the sources of these hydrocarbons.

3. Methods and Dataset

3.1. Methods

Burial and thermal history modeling (thermal maturity modeling) was performed by applying the 1-D PetroMod software (Schlumberger, ver.9.0; for details see [6,11]). Applied numerical modeling techniques permit the simulation of the complex set of interacting physical and chemical processes that took place during the evolution of a sedimentary basin. A starting point for the modeling is a conceptual model [6,11], which describes the geological evolution of the study area, including geological, geophysical, and geochemical data. A discretized numerical model, which represents the conceptual model, is then used for simulation purposes [6,11]. The geological history for a single well section is calculated using the finite difference method. Geological events, scaled in time, create the framework of a model and govern the data input. The data set for each event consists of duration, depositional or erosional thickness, lithology, bathymetry, sediment/water interface or surface temperature, and heat flow. Petrophysical parameters, such as porosity, density, and thermal conductivity, are then defined on the basis of lithology. After each simulation run, the calculated results have to be compared with the measured values to calibrate the model and check its geological reliability. Calibration is usually performed by varying the paleo-heat flow or the original thickness of the now-eroded sedimentary units [6,11]. Initially, heat flow estimates for the past stages of the basin history are assigned on the basis of the tectonic setting [6]. In the subsequent iterations, the paleo-heat flow values are adjusted through the modeling procedure to achieve the best fit between the calculated model and the measured calibration parameters. Heat flow values are best constrained for times of maximum temperature, which correspond to the maximum burial in many cases [6]. The backstripping method, which also includes a decompaction correction, was applied to establish the burial history. Petrophysical parameters were used based on the PetroMod library according to lithology types identified in the analyzed wells [64]. Models were calibrated using present-day corrected borehole temperature data [35] and measured values of mean random vitrinite reflectance [47,52,65]. VR in PetroMod modeling was calculated using the algorithm of Sweeney and Burnham [66]. Several tests of the change of heat flow over time, erosion/exhumation of overburden, and a combination of both were performed. The calculated VR value was compared with the measured VR value, and the model was adjusted until the best fit of the VR versus depth was achieved. A broader discussion of the applied maturity modeling method is provided elsewhere [6,11,54].

3.2. Dataset and Input Data

The Pilzno-40 well was drilled during hydrocarbon exploration by the Polish Oil and Gas Company (PGNIG) in 1991. The borehole reached a total depth of 3733 m; its geographical coordinates are 49°58′44,57″ N and 21°19′38,82″ E. In the study area, a small natural gas field occurs in the Miocene strata [49,55,67]. Stratigraphic succession of the Pilzno-40 well includes (Figure 3) a few meters of Quaternary sediments, below flysch deposits of the Skole Unit and folded Miocene of the Zgłobice Unit, autochthonous Miocene, marls of the Cretaceous, limestones of the Upper Jurassic, sandstones of the Lower Triassic, black shales of the Silurian (Wenlock), and carbonates of the Ordovician (Llandeil-Caradocian) strata [49,55,67].

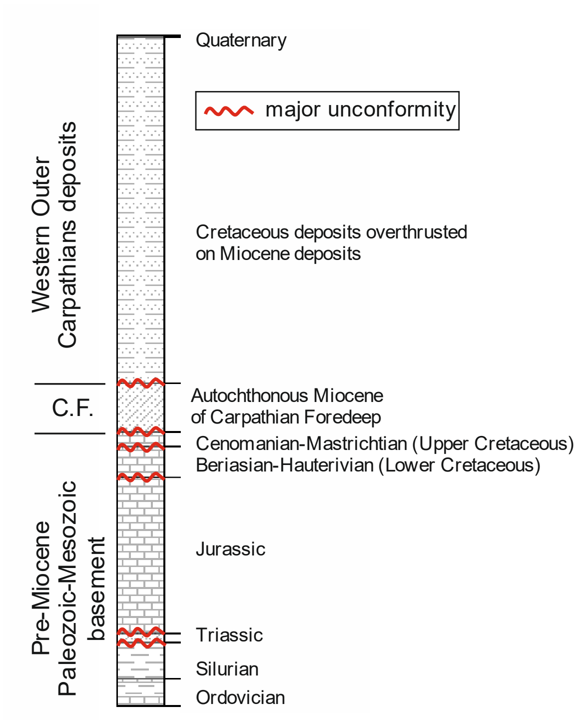

Figure 3. Stratigraphic column of the Pilzno-40 well. Below the very thin Quaternary sediments, there are flysch deposits of the Skole Unit, which consist of shales (siltstones) and sandstones that represent the Inoceramus Beds of the Upper Cretaceous. The flysch strata are thrust over the sandy-clayey Miocene series (Upper Badenian) of the Zgłobice Unit. The pre-Miocene basement consists of epicontinental Cretaceous marls resting on Upper Jurassic marls and limestones. Below the Jurassic, there are clastic sandy-clayey beds of the Lower Triassic (Buntsandstein-middle part), which in turn rest on Silurian graptolitic shales (Wenlock) and Ordovician (Llandeil-Caradocian) carbonates [49,65,67]. C.F. Carpathian Foredeep. Note that several significant unconformities occur in the sedimentary succession of the study area. These represent periods of substantial erosion.

In the Pilzno-40 well, the VR dataset includes only four samples from the Jurassic and Paleozoic (Figures 3–6). VR versus depth plot shows a small VR increase, from ca. 0.64% in the Jurassic to up to 0.69% in the Paleozoic. However, single organic particle VR measurements in each sample scatter between ca. 0.5 and 0.8% [47,48]. These average VR values are fully supported by other geochemical thermal maturity data from T_{max} Rock-Eval and the dibenzotiophene index [47]. Thermal maturity in the Pilzno-40 well shows that both Jurassic and Silurian organic matter is in an early mature phase for hydrocarbon generation (early oil window), which is consistent with the maturity profile in adjacent wells in the study area [48,53]. Oil-prone type-II kerogen occurs in Ordovician and Silurian rocks. The initial TOC equals 2.6% in the Silurian and 1.1% was assumed in the Ordovician based on adjacent wells [47]. The organic matter in Jurassic rocks, containing gas-prone type-III kerogen with an admixture of type-II kerogen, is usually immature in Upper Jurassic strata or, at most, early mature to 0.7%VR in Middle Jurassic strata in the entire study area. In the Pilzno-40 well, a succession similar to the thermal maturity is observed of ca. 0.64 to 0.67%VR. However, Upper Jurassic sediments usually contain below 0.5% TOC [53]. The above-mentioned geochemical characteristics were applied to the petroleum generation in this modelling.

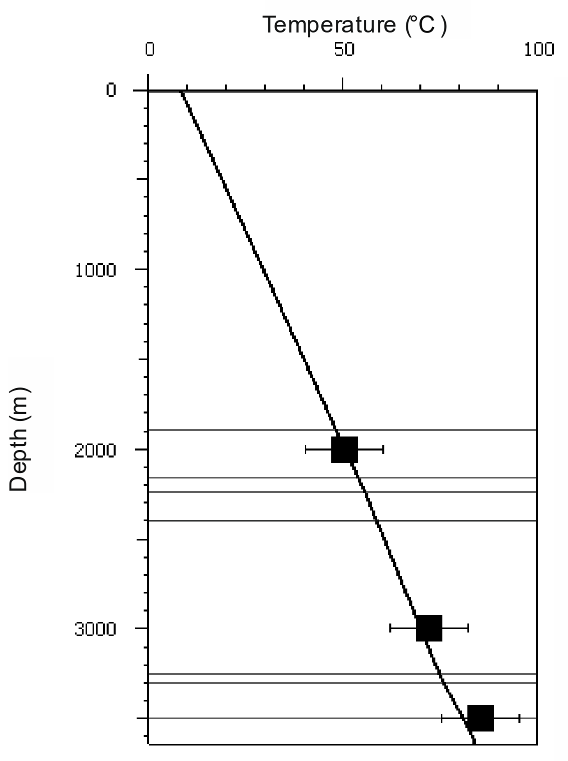

Figure 4. Calculated temperature curve using PetroMod software vs. measured data from [34].

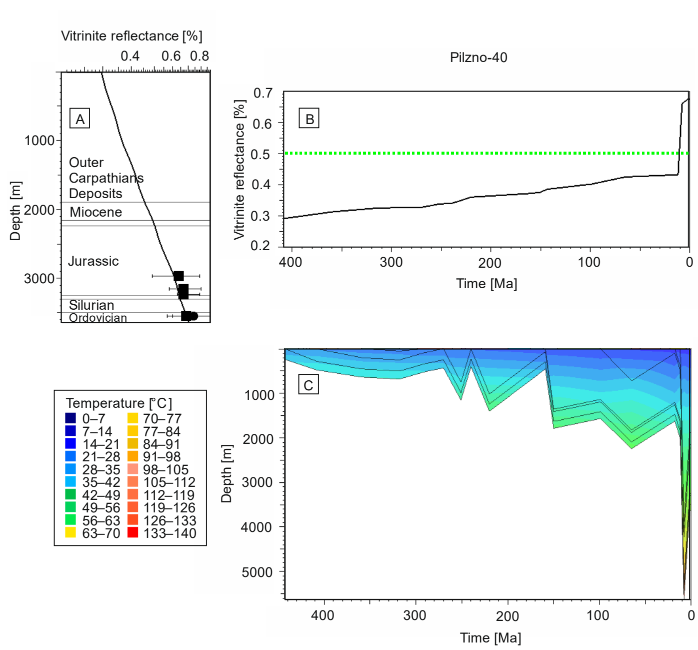

Figure 5. Burial and thermal history model (no. 1) for the Pilzno-40 well assuming Late Miocene overthrusting of the Outer Carpathians: (**A**) calibration of the model by comparison between measured VR values and calculated VR curve; (**B**) VR evolution with time showing a rapid increase due to the Carpathian overthrust. The green dash line is the VR value equals 0.5% that represents border between immature and mature kerogen; (**C**) burial history curves with temperature overlay. Note the fast temperature increase in the late Miocene.

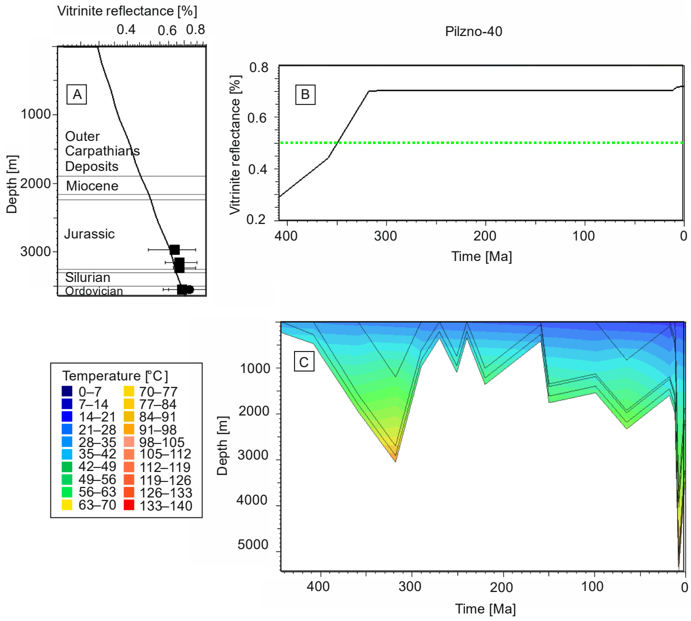

Figure 6. Burial and thermal history model (no. 2) for the Pilzno-40 well assuming Late Miocene overthrusting of the Outer Carpathians but with Variscan burial heating: (**A**) calibration of the model by comparison between measured VR values and the calculated VR curve; (**B**) VR evolution with time showing a major increase in the Devonian–Carboniferous, whereas the Miocene overprint is not particularly important. The green dash line is the VR value equals 0.5% that represents border between immature and mature kerogen; (**C**) burial history curves with temperature overlay. Note the temperature increase, first in the Carboniferous, and later in the Late Miocene.

The average present-day geothermal gradient in the Pilzno-40 area is 22 °C/km [35]. A similar present-day thermal field was also found in adjacent areas [35,68]. The surface temperature was set automatically using the SWIT tool, which extracts a standard temperature at sea level over geological time for any given location, based on the model of Wygrala [69]. The present-day surface average temperature is 9 °C. We did not consider the paleo-water depth because the predominant influence on the thermal evolution is exerted by sediment thickness, e.g., [70], as most of the sedimentation in the study area occurred in platform shallow water environments that did not exceed 200 m [40–50].

In the Pilzno-40 well succession, a significant stratigraphic unconformity occurs between Lower Silurian and Lower Triassic strata (Figure 3). The next important unconformity occurs between the Lower Triassic and Middle-Upper Jurassic, and between the Lower and Upper Cretaceous, and between the Upper Cretaceous and Miocene. These gaps in the sedimentary record allow different hypotheses to be assumed regarding the burial history of the study area, as discussed below.

4. Results

Using PetroMod software (version 9.0, one-dimensional 1–D, Schlumberger, Houston, TX, USA), the present-day heat flow value was calculated to be 56 mW/m^2 based on fitting to the present-day temperatures measured in the borehole (Figure 4).

A short but linear VR profile (Figures 5–9) suggests a burial-driven diagenesis of organic matter. If the pre-Triassic heating was responsible for the thermal maturity of the Paleozoic samples, it should be possible to observe a jump of VR gradient between Lower Silurian and Triassic data when VR vs. depth is plotted. However, due to the very limited Silurian samples (only one), a clear determination is not possible of the nature of the temperature change in the Pilzno-40 section; thus, no distinction between Mesozoic and Paleozoic thermal evolution can be conducted.

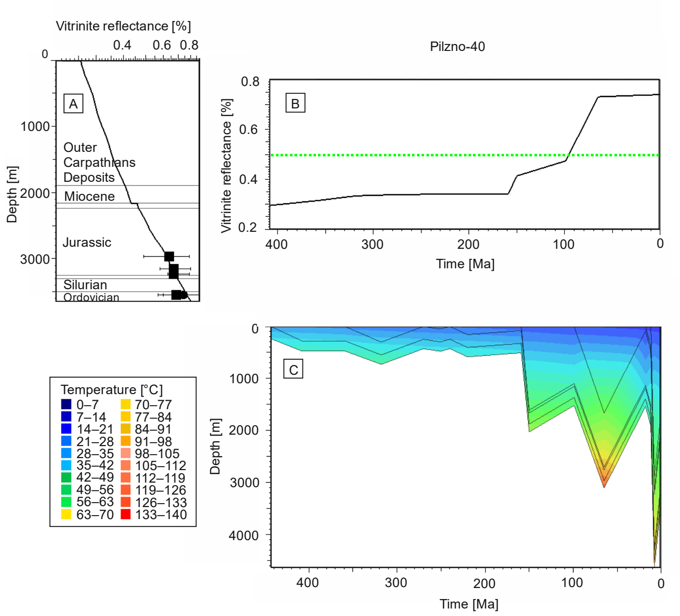

Figure 7. Burial and thermal history model (no. 3) for the Pilzno-40 well assuming Late Miocene overthrusting of the Outer Carpathians but with Jurassic–Cretaceous burial heating: (**A**) calibration of the model by comparison of measured VR values and calculated VR curve; (**B**) VR evolution with time showing a major increase in the Jurassic–Cretaceous, whereas the Miocene overprint is not particularly important. The green dash line is the VR value equals 0.5% that represents border between immature and mature kerogen; (**C**) burial history curves with temperature overlay. Note the temperature increase first in the Jurassic–Cretaceous and later in the Late Miocene.

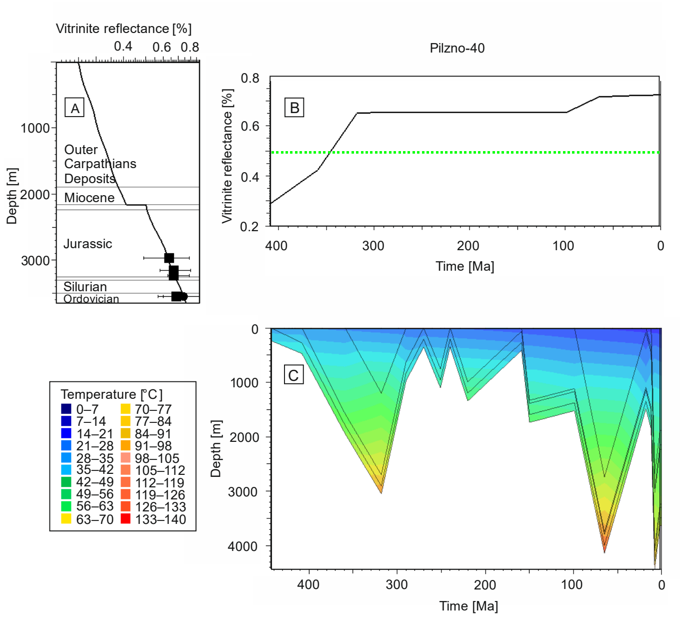

Figure 8. Burial and thermal history model (no. 4) for the Pilzno-40 well assuming Late Miocene overthrusting of the Outer Carpathians but with 2500 m Cretaceous and Variscan burial heating: (**A**) calibration of the model by comparison of measured VR values and calculated VR curve; (**B**) VR evolution with time. The green dash line is the VR value equals 0.5% that represents border between immature and mature kerogen; (**C**) burial history curves with temperature overlay. Note the temperature increase first in the Devonian–Carboniferous, then the Cretaceous, and, finally, the Late Miocene.

Thermal maturity models were developed to account for all known parameters and assumptions described above and constrained with thermal maturity and well temperature data (Figures 5–9 and Table 1). Parameters that were varied were those that exerted a first-order influence on thermal development, such as maximum burial and heat flow. These were adjusted iteratively to obtain the best possible fit to the constraints. During the modeling, it became obvious that varying only a single model input (e.g., only heat flow) would not provide an acceptable fit. Consequently, a number of different combinations of parameters, such as the maximum subsidence, or the variation of the maximum heat flow value and its length, were considered in numerous model iterations to determine the scenario with the best fit to the thermal maturity data. As shown in Figures 5–9, several good thermal models were able to be developed, which were all able to satisfy the measured VR data in the given well sections. Thus, the comparison between the models shown in Figures 5–9 emphasizes the necessity to cross-check this kind of reconstruction with different paleotemperature indicators (mineralogical and geochemical), thermochronological data, and geological constraints.

Table 1. Basic assumption in the analyzed models.

Model Number	Pre-Miocene Major Burial Event	Age of Max. Burial (Ma)	Miocene Burial Stage *	Heat Flow (mW/m^2)	Erosion (m)
1	No	10	Yes	47	2000
2	Devonian-Carboniferous (Variscan)	320	Yes	62	1500 Devonian and 1200 Carboniferous
3	Jurassic-Cretaceous	65	Yes	62	500 Jurassic, 800 Cretaceous
4	Cretaceous	65	Yes	62	500 Jurassic, 2500 Cretaceous
5	Latest Triassic	205	Yes	120	1500

* Miocene burial stage is due to tectonic burial caused by the Outer Carpathians, and it is assumed in each of the five models. However, in models 2–5, pre-Miocene burial events are also assumed to be possible. Heat flow value given for maximum burial time.

In the first model (no. 1) of burial and thermal history, it was assumed that the Carpathian overthrust has a major influence on thermal maturity of the Pilzno-40 section (Figure 5). Erosion/exhumation of the Carpathian flysch was assumed for 2 km based on thermochronological findings in the adjacent area [34,70]. The heat flow was 62 mW/m^2 from the Ordovician to early Miocene, before subsequently decreasing to the maximum tectonic burial due to Carpathian load (up to 47 mW/m^2), and slightly increasing to the present-day value of 56 mW/m^2. Consequently, rapid deposition of molasse sediment caused a downward deflection of the isotherms, e.g., [71], which is typical of foreland basins. Then, the heat flow increased immediately during the inversion phase. Pre-Miocene thermal evolution is negligible, because, in such a model, thermal maturity is related directly to maximum burial and maximum temperature reached during Miocene tectonic burial. This model showed good calibration of thermal maturity (calculated VR curve vs. measured VR values). Thermal maturity, both for Jurassic and Silurian strata, achieved its maximum value in the Late Miocene (Figure 5).

In a further attempt to derive a suitable solution, a number of other models (no. 2–5) were constructed, assuming several different scenarios of pre-Miocene tectono-thermal evolution of the study area (Figures 6–8). In all of these models, the Carpathian overthrust influence was maintained as in model 1 from Figure 5. Heat flow evolution was assumed as in the first model for models 2–4 and elevated for model 5 (Table 1).

Model 2 assumed that 1500 m of Devonian and 1200 m of Carboniferous was eroded. This scenario was based on the geological evolution of adjacent areas [39–42]. The model showed a significant increase in VR in the Devonian to Carboniferous (Figure 6). Paleozoic burial reached its maximum at ca. 320 Ma. Permo–Mesozoic events that were too small to overprint earlier achieved thermal maturity, which was finally caused by the Carpathian overthrust. Thermal maturity calibration was also very good for such a model and is likely due to the influence of the Carpathian load. However, thermal maturation of Lower Paleozoic strata occurred in the pre-Permian period, whereas the maturity increase in the Late Miocene was negligible (Figure 6B).

The next model (no. 3) assumed important erosional events in the Jurassic (500 m) and Cretaceous (1800 m) (Figure 7). However, this model appears to be less probable considering geological evolution of the study area [39–42]. This model also allows for proper calibration. In this model, thermal maturity was achieved in the Late Mesozoic. The further combination of models (no. 4) assumed burial in the Devonian and Carboniferous, in addition to additional burial in the Late Cretaceous (Figure 8). In this model, good calibration was also observed; however, two stages of increase in thermal maturation occurred—first in the Carboniferous and then in the Cretaceous—whereas the Late Miocene increase was very small (Figure 8B).

The next model (no. 5) applied both heat flow and erosion as factors determining the thermal evolution of the study area (Figure 9). In addition to several tested erosional events related to major unconformities, an event between the Lower Triassic and Mid-Upper Jurassic can also be noted. According to Kiersnowski [72] and Moryc [48], the undivided Permian-Triassic sedimentary cover was much thicker and occurred in the entire area between Kraków and Rzeszów. Now, these sediments exist only in isolated tectonic structures, such as the Liplas–Tarnawa Trough. Moreover, Poprawa et al. [73] suggest that the Liplas–Tarnawa Trough developed as a pull-apart basin with a heat flow up to 100 to 150 mW/m^2 during its initial evolution origin. Therefore, in model no. 5, it was assumed that 1500 m of Triassic rocks were removed in the study area, and the heat flow was elevated to 120 mW/m^2 during this event (Figure 9). This model also allows for proper calibration. Moreover, the calculated maximum heating developed in the Latest Triassic to Early Jurassic, which is in accordance with illite K-Ar age (200 Ma) of Silurian bentonite in the adjacent Żukowice-39 well [74]. As the temperature during the Carpathian overthrust is similar to those of the Triassic–Jurassic, it appears that mineral and organic diagenesis developed in that period, whereas it was not overprinted by any later processes due to the Carpathian overthrust (Figure 9). As only this last thermal model was based on measurements (illite K-Ar age) related to the timing of thermal evolution in the study area, it was assumed to be the preferred model. In contrast, the other models were based only on the maximum exposure for heating (vitrinite reflectance) without directly constraining the timing of the processes by thermochronological data.

The performed maturity modeling allowed petroleum system elements to be established (Figure 10). The critical moment is the period that best depicts the generation and migration of hydrocarbons in a petroleum system, which is likely in the Latest Triassic to Early Jurassic (ca. 200 Ma) in the Pilzno-40 area. This is because the maximum heating occurred in that period. Due to the remigration hydrocarbons, which could have happened during the folding and uplifting of the Carpathians (ca. 10 Ma), a second critical period is possible. However, considering that hydrocarbon generation developed many millions of years before reservoir and trap formation, most hydrocarbons were dispersed and lost.

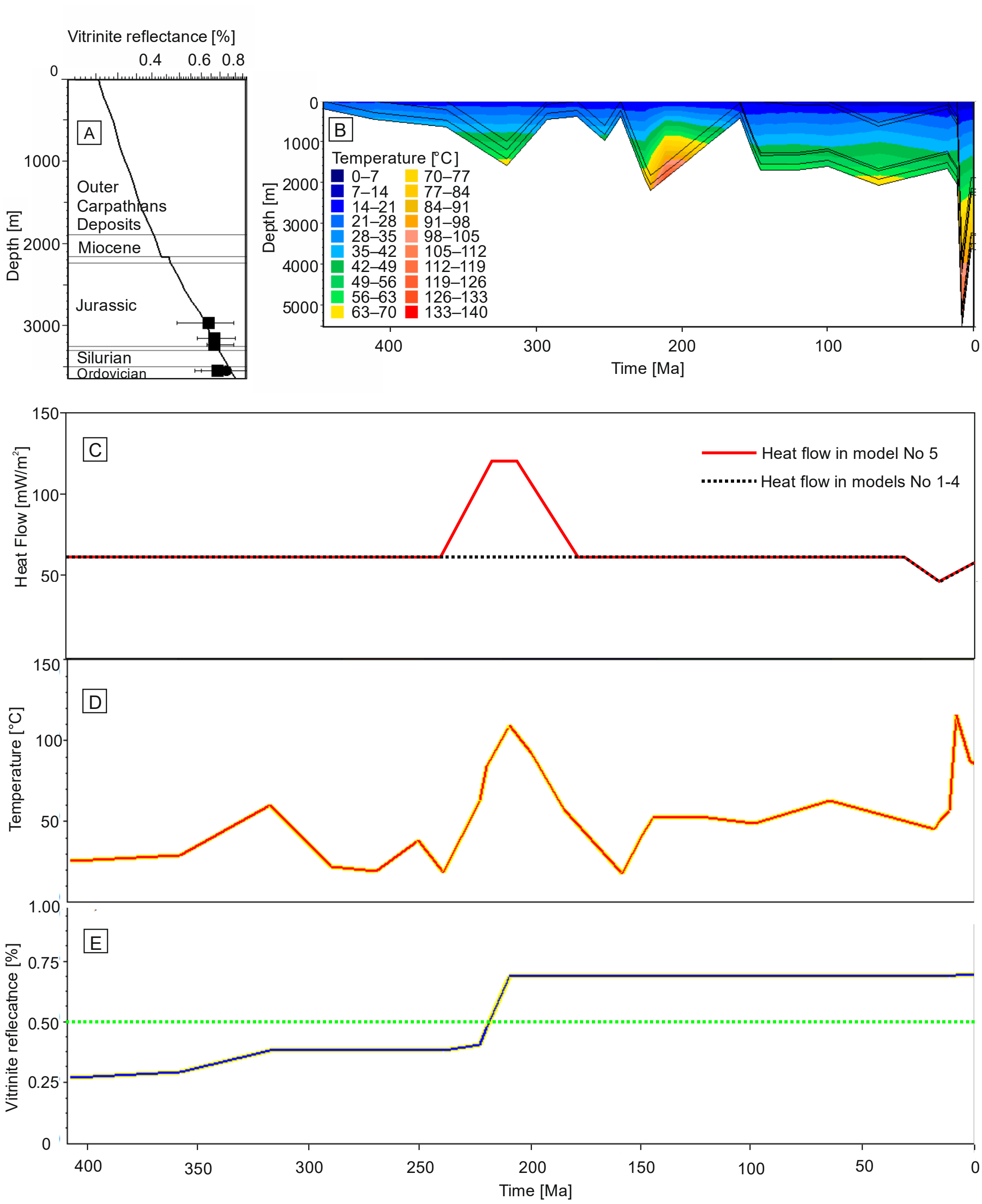

Figure 9. Results of maturity modelling for the Pilzno-40 well assuming that 1500 m of Triassic rocks were removed in the study area and heat flow was elevated to 120 mW/m^2 during the Latest Triassic. (**A**) Calibration of the model by comparison of measured VR values and calculated VR curve; (**B**) burial history curves with temperature overlay; (**C**) heat flow evolution; (**D**) temperature for top of Silurian strata in the Pilzno-40 well. Note that the maximum temperature of ca. 110 °C occurred in the Earliest Jurassic and also during the Carpathian overthusting in the Miocene. (**E**) Vitrinite reflectance evolution for Silurian strata applying model no. 5. The green dash line is the VR value equals 0.5% that represents border between immature and mature kerogen. A significant increase in VR developed in Late Triassic to Early Jurassic. Therefore, hydrocarbon generation developed in that period. No particular VR overprint occurred in the Miocene. Such model diagenesis is supported by an illite K-Ar age of ca. 200 Ma from Silurian bentonite in the Żukowice-39 well [74].

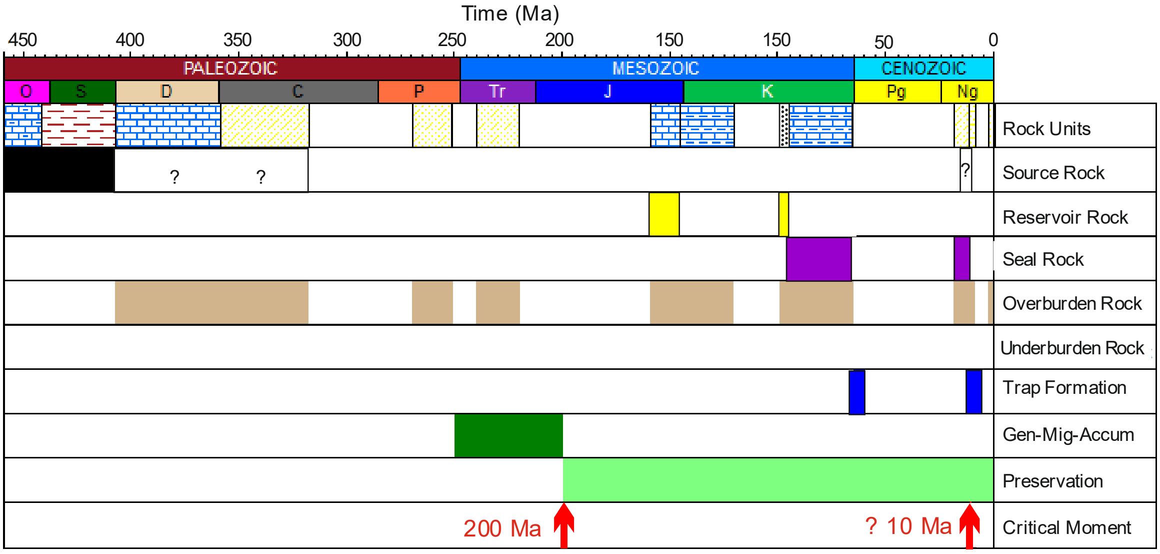

Figure 10. Petroleum system chart for study area. Sedimentary succession is not complete because it is divided by several significant unconformities. They likely represent periods of erosion of formerly deposited sediments. As a result, the burial history is not clear, and it is difficult to establish the timing of petroleum system events. Source rocks in the Pilzno-40 are Ordovician and Silurian strata; however, in adjacent areas, Devonian and Lower Carboniferous strata also include source rocks horizons. In the Outer Carpathians, Oligocene Menilite Shales are proven source rocks. In source rocks box the sign "?"means possible source rocks horizons. In Critical Moment box the sign "?"means the second possible critical moment due to hydrocarbon generation in the Oligocene Menilite Shales (ca. 10 Ma).

5. Discussion

5.1. Burial and Thermal History

The geothermal grade pattern in an accretionary wedge depends on the thermal structure of the associated subduction zone [75]. Accretionary wedges are usually associated with low geothermal gradients, particularly in the outermost part of the orogen. The geothermal gradient decreases in the wedge due to accretion of cold sediments [75,76]. However, fluid flow may locally increase the geothermal gradient. Based on the general pattern of geothermal gradients in accretionary wedges, the lowest paleogradient estimates are the most plausible for the actual amount of erosion, e.g., [75,76]. Heat flow successively decreases with the increase in sedimentary or tectonic burial, for example, during Miocene Carpathian thrusting, because the rate of heat flow decrease is proportional to the rate of subsidence [77].

Our calculated paleo-heat flow (47 mW/m^2) during maximum tectonic burial in the Late Miocene is lower than present-day heat flow values (56 mW/m^2); this result is consistent with similar results in the Alpine Molasse Basin in Austria, e.g., [7,78] and Switzerland [79]. These basins/areas have similar tectonic settings as the studied area of Pilzno-Tarnów because these basins belong to the entire Alpine–Carpathian System of fold-and-thrust belts with foredeep basins. The heat flow evolution of a continental collisional zone, which was similar to that of the Carpathians, was analyzed by Sachsenhofer [78] in the Eastern Alps, where heat flow during continental collision was extremely low (<40 mW/m^2) along the orogenetic front, whereas very high heat flow (>150 mW/m^2) occurred a few hundred kilometers south. The former was a result of crustal thickening and thermal blanketing due to rapid subsidence and sedimentation and nappe stacking. The latter was caused by slab break-off and magmatic activity [78]. The reconstructed low paleo-heat flow in Miocene resulted in low average paleogeothermal gradients, which reached ca. 25 °C/km in the autochthonous foreland and ca. 15 to 20 °C/km in the Outer Carpathians. The present-day average geothermal gradient of 26 °C/km in the Paleozoic basement of the Outer Carpathians is consistent with that of the study area [73]. Approximate paleogeothermal gradients inferred from methane–water fluid inclusions in quartz-calcite veins present in the Magura Nappe, and in the equivalents of the Dukla Nappe exposed in the Mszana Dolna and Szczawa tectonic windows, are 20 and 17 °C/km, respectively [80]. The fluid inclusions were related to regional collapse—the final stage in the structural evolution of the Outer Carpathian accretionary wedge [78,80]. The paleogeothermal gradients inferred from fluid inclusions are similar to the present-day gradient of 17 °C/km in the frontal part of the Outer Carpathians [73].

In the Polish part of the Outer Carpathians wedge, heating was mainly caused by Late Oligocene to Late Miocene tectonic burial resulting from crustal shortening and nappe stacking and was associated with a low to locally normal paleogeothermal gradient (16–26 °C/km) [76,80,81]. In the Carpathians, thermochronological data generally indicate that subsequent exhumation-related cooling occurred in several phases, mainly from ca. 30 to 5 Ma [70,81,82]. In the Ukrainian part of the Outer Carpathians, combined thermochronological and thermal maturity data showed that burial heating of the wedge reached ca. 170 °C in the central part of the thrust belt, whereas the outermost and innermost parts were heated to less than 60 °C and less than ca. 120 °C, respectively. Tectonic burial was less than 2 to 3 km in the outermost thrust sheets and in the foredeep [81], which is similar to that of the study area (1.5–2 km, compare in; [34]).

Tectonic burial due to Carpathian overthrusting in the Miocene did not reach 2 to 3 km in the outermost part of the orogen [34,70,81]. Slightly higher maximum values of tectonic burial of ca. 2 to 4 km, due to Carpathian load, could yield a temperature increase of ca. 30 to 60 °C at the top basement in the outermost areas of the Carpathians (i.e., in the study area). In addition, considering sediments with a thickness of ca. 1.5 km (Figure 3) up to the top of the Silurian would yield ca. 30 to 40 °C, depending of the geothermal gradient in the basement. Even assuming eroded Devonian and Lower Carboniferous strata of ca. 1.0 km, this could yield an additional ca. 20 °C. Combining the above temperature increases, this would finally result in a maximum temperature of up to ca. 120 °C at the top of Silurian strata during the Late Miocene. This is similar to the results of the performed modelling and is supported by the value of 0.7%VR (Figures 5–9) and 24% illite/smectite ratio [74]. A similar range of temperature could occur earlier in pre-Miocene evolution, e.g., in the Early Jurassic, as shown by illite K-Ar ages of Silurian bentonite in the Żukowice-39 well [74].

The results of the performed modeling exercises cannot be directly compared to other thermal modeling performed in the study area because almost all published models have not shown their calibration quality, i.e., measured VR data vs. calculated values [48,53,61,83]. However, all of this modelling shows the major influence of the Carpathian overthrust on thermal maturation in the Paleozoic–Mesozoic basement. The only exception is the thermal modelling results of Poprawa et al. [73] for the Tarnawa-1 well, which is located in the west of the study area in the Liplas–Tarnawa Trough. This tectonic structure is characterized by particularly thick Permian–Triassic sediments [72]. The clastic sediments of the undivided Permian–Triassic have been preserved in many places south and south-east of the Kraków area. Initially, they were located in a more extensive area, which later underwent multi-stage erosion. They have survived only in the areas originally constituting the axes of older Paleozoic synclines along the NNW–SSE direction, built from the Lower Carboniferous, and in some places, the Upper Carboniferous. These synclines were strongly dislocated by block tectonic movements in the Permian. At that time, numerous tectonic troughs with significant subsidence were developed. One of these is the Liplas–Tarnawa Trough, which is filled with Permian–Triassic sediments with a thickness of up to 1400 m [46,49,72]. Below the Permo–Triassic succession, Devonian and Carboniferous strata are present, which are not present in the Pilzno-40 section. In the Tarnawa-1 well, the thermal maturity for the autochthonous Miocene is 0.45 to 0.48%VR, and 0.6%VR in the Jurassic, which is similar to that in the Pilzno well area. The VR in the Carboniferous is 0.7 to 0.85%, whereas in the Devonian it is 0.72 to 0.96%. The results of maturity modelling in the Tarnawa-1 well suggest that a short-term Late Permian to Early Triassic heat flow (ca. 100 to 150 mW/m^2) anomaly occurred due to pull-apart tectonic development [73].

Additionally, along the Krakow–Lubliniec Fault Zone, magmatic activity could cause an increase in heat flow, which may be an alternative explanation of this heat flow anomaly. The Krakow–Lubliniec Fault Zone contains numerous igneous intrusive rocks that are the products of bimodal magmatism and developed during two major Variscan phases. The older magmatism is related to extensional faults in the basement of the Moravo–Silesian foreland. The younger, Latest Carboniferous to Early Permian, more intense magmatic activity is known only along the eastern border of the Upper Silesia Coal Basin and on the Małopolska Block, e.g., ([84] and references therein). Similar to the case of the Liplas–Tarnawa area, a thermal history model was also proposed by Dudek et al. [45] for the area to the north, i.e., Bochnia-Grobla, which emphasized a Late Paleozoic to Early Mesozoic maximum heating and petroleum generation in several stages for the given source rocks. Therefore, in the Liplas–Tarnawa Trough, two stages in the thermal history can be distinguished: the older stage with a warmer thermal regime and the younger stage with a cooler thermal regime. First, the Devonian and Carboniferous deposits and the lower part of the Permian sediments were heated, then the thermal maturity of the sediments of the Upper Permian, Mesozoic, and autochthonous Miocene developed [45,73]. However, a constant heat flow option cannot be completely ruled out. After the Late Carboniferous and before the Middle Jurassic, a thermal event occurred in the study area, which may have been related either to the heating resulting from the development of the Liplas–Tarnawa pull-apart basin or to the magmatic activity along the Krakow–Lubliniec Fault Zone. Later, in the Miocene, the thermal structure was disturbed due to the overlapping of relatively cool deposits of the Outer Carpathian orogen, and the process of rebuilding the thermal equilibrium as a result of this event continues to the present [73].

Considering the more likely model of heating associated with the development of the pull-apart basin, the potential source rocks of the Paleozoic could have achieved the thermogenic hydrocarbon generation phase in the Permian–Triassic, whereas during the Miocene, tectonic burial could only slightly reactivate the generation process. With the adoption of a less probable model, in which heat flow is constant over time, the above-mentioned processes reached generation phases in the Late Miocene. In the more likely Variscan or pull-apart heating model, any generated hydrocarbons were dispersed in the Late Triassic to Early Jurassic, and/or in the Paleogene, due to the lack of regional sealing [73]. To summarize, in the study area, an Early Mesozoic thermal event caused hydrocarbon generation in Paleozoic source rocks, and no overprint occurred later in the Miocene.

The relatively low thermal maturity of Carboniferous strata under the Carpathian overthrust and a coal rank pattern similar to that of the more northern part of the Upper Silesian Coal Basin not covered by the Carpathians, e.g., [85], in addition to thermal modelling results [86,87], show that the Carpathian overthrust and development of the Carpathian Foredeep in the Miocene was most likely too small to reinitiate further thermal maturation and petroleum generation in either the Czech [87] or Polish parts of the Upper Silesian Coal Basin [86].

In the Ukrainian region, the autochthonous foreland is part of the SW margin of the East European Platform and is partially overthrust by the Carpathian orogen. Sedimentary succession belonging to several different sedimentary cycles occurs there. Pre-Mesozoic rocks in the foreland are overmature, at least within the central and SE parts of the study area. Therefore, petroleum accumulations in this area are probably confined to the Mesozoic–Cenozoic sedimentary cover [88].

5.2. Implications for Petroleum Exploration

The easiest apparent interpretation of burial and thermal history in the study area is the assumption of a dominant role of the Carpathian overthrust over foreland. In such a case, tectonic load may have caused an increase in subsidence and burial, and in temperature in rocks below the overthrust [73,89,90]. Alternatively, a two-stage process is possible, comprising some increase in pre-Late Jurassic and further development under the Carpathian overthrust in the Miocene, e.g., [48]. It is rarely assumed that pre-Jurassic hydrocarbon generation was a major phase of these processes [46,73]. However, Paleozoic strata occur in very limited areas of the Małopolska Block [40]. The pre-Silurian erosion is well marked in the whole study area because various Ordovician levels are present under the Silurian deposits [67]. In addition, Variscan erosion must have been significant [43,46] because Devonian and Carboniferous strata are known, for example, in the west of the study area, whereas they do not occur in the Pilzno-40 area [40]. Limited occurrence of Permian and Triassic sediments is also known [49,72]. Therefore, a significant sedimentary record was removed by Caledonian, Variscan, and post-Variscan erosion [40,43,49,67]. The occurrence of Ordovician and Silurian sediments is particularly limited in the study area. Therefore, it is likely that the interval of the source rocks located within them were only locally able to generate hydrocarbons (if any) due to the Carpathian tectonic overburden.

The maximum paleotemperature for the top of Silurian strata, calculated from illite/smectite data, is ca. 125 °C, whereas the illite K-Ar age for Silurian bentonite is 200 Ma (Early Jurassic) in the Żukowice-39 well section [74]. Therefore, the maximum paleotemperatures of diagenesis of Silurian rocks likely occurred in the Latest Triassic to Early Jurassic in the study area, corresponding to thermal phenomena that were related to the breakup of Pangea and an enhanced heat flow related to the opening of the North Atlantic, e.g., ([91] and references therein). Contemporary, rapid burial-driven diagenesis that occurred due to development of a pull-apart Liplas–Tarnawa trough and/or other transtensional processes may also be related to these regional phenomena. Such a tectonic regime implies that both factors—high heat flow and rapid burial—contributed to diagenesis development. Moreover, the temperature of 125 °C can be transferred into a VR scale, resulting in values of ca. 0.7%, which are typical for the top of the Silurian in study area, including the Pilzno-40 area [47,48]. This compatibility between organic diagenesis and mineral diagenesis suggest that these processes were mainly caused by burial heating. Therefore, the thickness of Triassic or Permo–Triassic sediments would have been much higher. However, these sediments survived only in some troughs, such as Liplas–Tarnawa [49,72]. This maximum heating event caused major phase hydrocarbon generation in Paleozoic source rocks.

Oils in the deposits of the Paleozoic–Mesozoic foreland are very similar to Carpathians thrust-belt oils, having a light to medium character, with densities of 0.81 to 0.86 g/cm^3 and paraffin content of 2 to 9% [89]. Based on geochemical source rock characteristics, possible source rock candidates for the described fields in orogenic foreland are: Ordovician, Silurian, Middle-Upper Devonian, Lower Carboniferous of the foreland, and Oligocene Menilite shale thrust-belt strata [38,47]. All of these source rocks are characterized by the quantity, quality, and maturity of organic matter that allowed the generation of the analyzed oils [47]. The oil/source rock correlation for hydrocarbon fields, e.g., Grobla, Partynia-Podborze, and Tarnów, indicates that oils from the autochthonous foreland are characterized by the presence of 28, 30-dinorhopane, oleanane, and highly branched C-25 isoprenoid alkane [55]. In addition, in the Czech part of the Carpathian Foredeep, these biomarkers have been identified [92]. The unequivocal identification of oleanane and related angiosperm-derived biomarkers indicates that the effective source rock has a Late Cretaceous-Cenozoic age [93–95]. Więcław et al. [47] and Kotarba et al. [38] assumed that oleanane in these oils is most likely to be sourced from the Upper Cretaceous rocks and/or the Miocene strata sealing rocks. Więcław [96] supposed that oleanane was likely eluted from Cretaceous rocks during the migration of hydrocarbons from Paleozoic source rocks. Considering that Upper Cretaceous carbonates contain a very low amount of organic matter, such an elution mechanism seems to be impossible; in particular, Paleozoic oils would have only migrated through fault systems directly into Cenomanian sandstones. The contamination of the oil with this biomarker in the sandstone reservoir condition is rather unlikely in this case. However, generation of these oils by the Oligocene Menilite Shales was also accepted by Więcław et al. [47] as an alternative explanation because it cannot be clearly excluded. It should be noted that Upper Cretaceous rocks sealing the Grobla deposit are carbonates, which are very poor in organic matter; therefore, the admixture from them is doubtful, and the Miocene is not directly sealing the oilfield. Therefore, hydrocarbons in Grobla and adjacent oil fields likely come from the Menilite Shales.

High sulfur content in oils can be related to high sulfur type-II kerogen documented in the lower Menilite Beds [55–57], which excludes Ordovician–Silurian source rocks. Due to this sulfur content, kerogen was able to generate oil much earlier and faster than typical low-S-II type [56,57]. Thus, it appears that the Lower Menilite Shales [55–57] are the main source of these oils, because Menilite Shales kerogen is mature in the Dukla Unit and in deep synclines of the Silesian Units [38,54,62]. Therefore, it appears that, as shown by Nemčok and Henk [63] based on numerical modeling, hydrocarbons migrated from the Menilite Beds to the foreland. Moreover, hydrothermal quartz from mineralized joints of the Outer Carpathians contains numerous fluid inclusions, which indicate the migration of hot (above 200 °C) methane-rich fluids from over-pressured sediments with fluid pressures of 50 to 300 MPa [80]. Hydrocarbons generated in the Menilite Beds were squeezed and migrated and filled a few traps in the basement of the Carpathian Foredeep. In contrast, further to the N and NW or NE, this migration did not occur. Therefore, no hydrocarbon accumulations exist further from the frontal Carpathians thrust (Figure 1). In Paleozoic source rocks, hydrocarbon generation developed mainly in pre-Jurassic times. A similar thermal phase was also identified in Carboniferous strata in the Fore-Sudetic Homocline [97], confirming earlier thermal modeling results [98].

In the study area, the major petroleum reservoir horizon is Cenomanian sandstone has a thickness of up to ca. 120 m (Figure 10). Considering the very limited occurrence of Silurian and Ordovician source rocks, which likely generated hydrocarbons in pre-Middle Jurassic phases, it appears unlikely that they could contribute to the charge of these Late Jurassic and Cenomanian petroleum fields (Figure 11) because, during hydrocarbon generation, no reservoir and traps or sealing existed. It is worth noting that the Cenomanian reservoir extends to the south below the Carpathian overthrust, which may have been charged by the Menilite Shales.

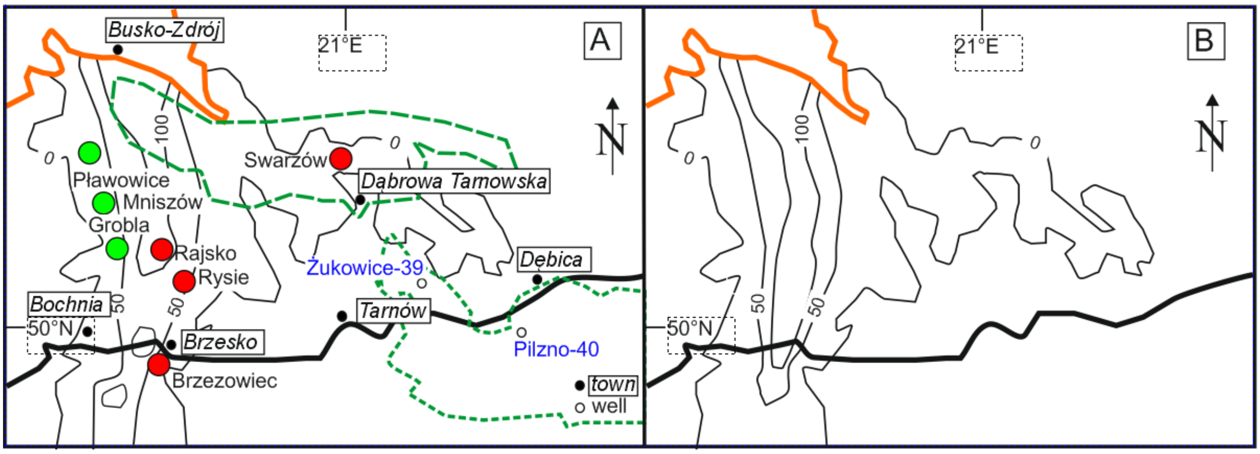

Figure 11. Simplified maps of: (**A**) distribution of oil (green dots) and gas (red dots) fields in reservoirs of Cenomanian sandstones [4], on the thickness (in m) of Cenomanian strata [35]. Dark green lines show the pattern of the Ordovician–Silurian source rocks [40]. (**B**) Hydraulic conductivity (in $m^3/s \times 10^{-5}$) in Cenomanian sandstones [35]. The orange line shows the northern extent of the Miocene sediments. The bold black line shows the northern occurrence of the Outer Carpathians. Note that the southern extent of Cenomanian sandstones is under the Outer Carpathians. Hydraulic conductivity values increase with the thickness of Cenomanian sandstones.

Picha [2] postulated that one of the many factors affecting thin-skinned thrust belts and their foreland is late orogenic normal, reverse, and strike-slip faulting, which occurs in the foreland and sometimes extends into the overlying thin-skinned thrust belts. These processes are active during the late phases of convergence, when subduction-driven thin-skinned thrusting ceases, and the remaining convergence and geometric adjustment occur mainly within the foreland plate [2]. As major petroleum generation and migration in both the thrust belt and the foreland usually occur in the late orogenic phase, this faulting could influence the development of migration pathways, particularly in the outermost part of the fold-and-thrust belt, as in the study area in the Carpathians. In the Austrian part of the Alpine fold-and-thrust belt, hydrocarbon migration from sub-thrust Oligocene source rocks into the undeformed foreland Cenomanian reservoirs by the fault system has also been emphasized [7]. The possibility of filling the reservoirs in the Mesozoic basement with the hydrocarbons generated within the Carpathian flysch strata suggests that other structures similar to the Ukrainian Lopushna field may have accumulated hydrocarbons, and that new discoveries of such fields are possible [99].

Generally, Paleozoic source rocks were subjected to several heating/cooling phases due to burial and tectonic inversion that occurred in the Late Paleozoic and Mesozoic. Therefore, it appears that during the Miocene Carpathian tectonic burial, Paleozoic source rocks were almost completely exhausted and unable to generate hydrocarbons. In terms of petroleum exploration, the modeling exercise and geological consideration presented here has important implications for the timing of maturation of Paleozoic source rocks in the study area. If Paleozoic source rocks are present, they will make a significant contribution to the hydrocarbon charge only in those areas that experienced relatively low heat flow and low burial during the pre-Middle Jurassic period, and where sufficient Late Jurassic–Cretaceous or Carpathian overthrust in Miocene burial has occurred to subsequently expose the kerogen to higher temperatures. Any scenario, however, is difficult to prove without additional mineralogical, geochemical, and, in particular, thermochronological research of the Paleozoic–Mesozoic basement.

6. Conclusions

The following conclusions can be drawn based on the thermal maturity modeling results:

- Tectono-thermal evolution excludes Paleozoic source rocks of the foreland from being an effective and important source rock for many Mesozoic petroleum fields in the autochthonous foreland, at least in the study area.
- In the frontal Carpathian orogenic wedge, the Paleozoic source rocks in the basements likely reached maximum heating in the Late Triassic to Early Jurassic period, which caused a major phase of hydrocarbon generation.
- The hydrocarbon potential of Paleozoic source rocks was exhausted before Upper Jurassic and Cenomanian reservoir rocks and traps were formed. Consequently, the majority of hydrocarbons generated during the pre-Jurassic stages were lost. Thus, it can be concluded that the hydrocarbons contained in Mesozoic reservoirs were charged by younger source rocks, i.e., occurring within the Outer Carpathians, such as the Oligocene Menilite Shales.
- This work shows that more comprehensive mineralogical, geochemical, and, in particular, thermochronological research of the Paleozoic–Mesozoic basement is necessary for petroleum system analysis in this region. In particular, explanation of pre-orogenic evolution is crucial for establishing effective source rocks for hydrocarbon charge in Mesozoic reservoirs. Combined with seismic data, this would likely help in hydrocarbon exploration in the pre-Miocene basement of the Carpathian Foredeep.

Funding: This work was supported by a statutory works—subvention no. 16.16.140.315 from the AGH University of Science and Technology.

Data Availability Statement: All data are included in the paper.

Acknowledgments: The author sincerely thanks Jan Golonka (AGH, Kraków) for the encouragement to publish this research, István Dunkl (Göttingen University, Germany) for inspiration to think outside the box, and Chris Clayton (CCGS, Tenbury Wells, Worcestershire, UK) for discussion on various aspects of organic geochemistry. Three anonymous reviewers are also thanked for their valuable input, which improved the quality of the paper, and the journal editors for help and efficient work.

Conflicts of Interest: The author declares no conflict of interest.

References

1. Picha, F.J. Exploring for hydrocarbons under thrust belts a challenging new frontier in the Carpathians and elsewhere. *AAPG Bull.* **1996**, *89*, 1547–1564.
2. Picha, F.J. Late orogenic faulting of the foreland plate: An important component of petroleum systems in orogenic belts and their forelands. *AAPG Bull.* **2011**, *95*, 957–981. [CrossRef]
3. Ślączka, A.; Kruglov, S.; Golonka, J.; Oszczypko, N.; Popadyuk, I. Geology and hydrocarbon resources of the Outer Carpathians, Poland, Slovakia, and Ukraine: General Geology. In *The Carpathians and Their Foreland: Geology and Hydrocarbon Resources*; Golonka, J., Picha, F.S., Eds.; AAPG Memoir: Washington, DC, USA, 2006; Volume 84, pp. 221–258.
4. Górka, A.; Gliniak, P.; Madej, K.; Maksym, A. Oil and gas fields in the Carpathians and the Carpathian Foredeep. *Przegląd Geol.* **2007**, *55*, 993–998, (In Polish with English Summary).
5. Mukhopadhyay, P.K. Maturation of organic matter as revealed by microscopic methods: Applications and limitations of vitrinite reflectance, and continuous spectral and pulsed laser fluorescence spectroscopy. *Dev. Sedimentol.* **1992**, *47*, 435–510.
6. Hantschel, T.; Kauerauf, A. *Fundamentals of Basin and Petroleum Systems Modeling*; Springer: Heidelberg, Germany, 2009; p. 436.
7. Gusterhuber, J.; Hinsch, R.; Linzer, H.G.; Sachsenhofer, R.F. Hydrocarbon generation and migration from sub-thrust source rocks to foreland reservoirs: The Austrian Molasse Basin. *Austrian J. Earth Sci.* **2013**, *106*, 115–136.
8. Suchý, V.; Filip, J.; Sýkorová, I.; Pešek, J.; Kořínková, D. Palaeo-thermal and coalification history of Permo-Carboniferous sedimentary basins of Central and Western Bohemia, Czech Republic: First insights from apatite fission track analysis and vitrinite reflectance modelling. *Bull. Geosci.* **2019**, *94*, 201–219. [CrossRef]
9. Suárez-Ruiz, I.; Flores, D.; Filho, J.G.M.; Hackley, P.C. Review and update of the applications of organic petrology: Part 1, geological applications. *Int. J. Coal Geol.* **2012**, *99*, 54–112. [CrossRef]
10. Mählmann, R.F.; Le Bayon, R. Vitrinite and vitrinite like solid bitumen reflectance in thermal maturity studies: Correlations from diagenesis to incipient metamorphism in different geodynamic settings. *Int. J. Coal Geol.* **2016**, *157*, 52–73. [CrossRef]
11. Waples, D.; Kamata, H.; Suizu, M. The art of maturity modeling, part 1: Finding of a satisfactory model. *AAPG Bull.* **1992**, *76*, 31–46.
12. Castelluccio, A.; Andreucci, B.; Zattin, M.; Ketcham, R.A.; Jankowski, L.; Mazzoli, S.; Szaniawski, R. Coupling sequential restoration of balanced cross-section and low-temperature thermochronometry: The case study of the Western Carpathians. *Lithosphere* **2015**, *7*, 367–378. [CrossRef]
13. Csontos, L.; Nagymarosy, A.; Horváth, F.; Kováč, M. Tertiary evolution of the Intra-Carpathian area: A model. *Tectonophysics* **1992**, *208*, 221–241. [CrossRef]
14. Fodor, L.; Csontos, L.; Bada, G.; Györfi, I.; Benkovics, L. Tertiary tectonic evolution of the Pannonian basin system and neighbouring orogens: A new synthesis of palaeostress data. In *The Mediterranean Basins: Tertiary Extension within the Alpine Orogen*; Durand, B., Jolivet, L., Horváth, F., Séranne, M., Eds.; Geological Society: London, UK, 1999; Volume 156, pp. 295–334.
15. Picha, F.J.; Stránik, Z.; Krejci, O. Geology and hydrocarbon resources of the Outer Western Carpathians and their foreland, Czech Republica. In *The Carpathians and Their Foreland: Geology and Hydrocarbon Resources*; Golonka, J., Picha, F.J., Eds.; AAPG Memoir: Washington, DC, USA, 2006; Volume 84, pp. 49–175.
16. Nemčok, M.; Krzywiec, P.; Wojtaszek, M.; Ludhová, L.; Klecker, R.A.; Sercombe, W.J.; Coward, M.P. Tertiary development of the Polish and eastern Slovak parts of the Carpathian accretionary wedge: Insights from balanced cross sections. *Geol. Carpath.* **2006**, *57*, 355–370.
17. Golonka, J.; Oszczypko, N.; Ślączka, A. Late Carboniferous-Neogene geodynamic evolution and paleogeography of the circum-Carpathian region and adjacent areas. *Ann. Soca. Geol. Pol.* **2000**, *70*, 107–136.
18. Golonka, J.; Gahagan, L.; Krobicki, M.; Marko, F.; Oszczypko, N.; Ślączka, A. Plate-tectonic evolution and paleogeography of the circum-Carpathian region. In *The Carpathians and Their Foreland: Geology and Hydrocarbon Resources*; Golonka, J., Picha, F.S., Eds.; AAPG Memoir: Washington, DC, USA, 2006; Volume 84, pp. 11–46.
19. Kováč, M.; Král, J.; Márton, E.; Plašienka, D.; Uher, P. Alpine uplift history of the Central Western Carpathians: Geochronological, paleomagnetic, sedimentary and structural data. *Geol. Carpath.* **1994**, *45*, 83–96.
20. Gągała, Ł.; Vergés, J.; Saura, E.; Malata, T.; Ringenbach, J.C.; Werner, P.; Krzywiec, P. Architecture and orogenic evolution of the northeastern Outer Carpathians from cross-section balancing and forward modeling. *Tectonophysics* **2012**, *532–535*, 223–241. [CrossRef]
21. Aleksandrowski, P. Structural geology of the Magura nappe in the Mt. Babia Góra region, western Outer Carpathians. *Studia Geol. Pol.* **1989**, *96*, 23–45, (In Polish with English Summary).
22. Decker, K.; Nescieruk, P.; Reiter, F.; Rubinkiewicz, J.; Ryłko, W.; Tokarski, A.K. Heteroaxial shortening, strike-slip faulting and displacement transfer in the Polish Carpathians. *Przegląd Geol.* **1997**, *45*, 1070–1071.
23. Decker, K.; Tokarski, A.K.; Jankowski, L.; Kopciowski, R.; Nescieruk, P.; Rauch, M.; Reiter, F.; Świerczewska, A. Structural development of Polish segment of the Outer Carpathians (Eastern part). Introduction to Stops: 7–16. Final Proca. In Proceedings of the 5th Carpathian Tectonic Workshop, Poprad, Slovakia, 5–9 June 1999; pp. 26–29.
24. Decker, K.; Rauch, M.; Jankowski, L.; Nescieruk, P.; Reiter, F.; Tokarski, A.K.; Galicia, T.G. Kinematics and timing of thrust shortening in the Polish segment of the Western Outer Carpathians. *Rom. J. Tecton. Reg. Geol.* **1999**, *77*, 24.
25. Świerczewska, A.; Tokarski, A. Deformation bands and the history of folding in the Magura nappe, Western Outer Carpathians (Poland). *Tectonophysics* **1998**, *297*, 73–90. [CrossRef]

26. Zielińska, M. Organic-matter vitrinite reflectance variability in the Outer Carpathians, Poland: Relationship to tectonic evolution. *Geol. Q.* **2017**, *61*, 214–226. [CrossRef]
27. Zielińska, M.; Fabiańska, M.; Więcław, D.; Misz-Kennan, M. Comparative petrography and organic geochemistry of different types of organic matter occurring in the Outer Carpathians rocks. *Geol. Q.* **2020**, *64*, 165–184. [CrossRef]
28. Waliczek, M.; Machowski, G.; Więcław, D.; Konon, A.; Wandycz, P. Properties of solid bitumen and other organic matter from Oligocene shales of the Fore-Magura Unit in Polish Outer Carpathians: Microscopic and geochemical approach. *Int. J. Coal Geol.* **2019**, *210*, 103206. [CrossRef]
29. Waliczek, M.; Machowski, G.; Poprawa, P.; Świerczewska, A.; Więcław, D. A novel VR_o, T*max*, and S indices conversion formulae on data from the fold-and-thrust belt of the Western Outer Carpathians (Poland). *Int. J. Coal Geol.* **2021**, *234*, No 103672. [CrossRef]
30. Oszczypko, N. The Western Carpathians Foredeep—Development of the foreland basin in front of the accretionary wedge and its burial history (Poland). *Geol. Carpath.* **1998**, *49*, 415–431.
31. Oszczypko, N. Development of the Carpathians Foredeep in Miocene. *Przegląd Geol.* **2001**, *49*, 717–723, (In Polish with English Summary).
32. Oszczypko, N. The structural position and tectonosedimentary evolution of the Polish Outer Carpathians. *Przegląd Geol.* **2004**, *52*, 780–791.
33. Krzywiec, P.; Bukowski, K.; Oszczypko, N.; Garlicki, A. Structure and Miocene evolution of the Gdów tectonic "embayment" (Polish Carpathian Foredeep)—New model based on reinterpreted seismic data. *Geol. Q.* **2012**, *56*, 907–920. [CrossRef]
34. Krzywiec, P.; Oszczypko, N.; Bukowski, K.; Oszczypko-Clowes, M.; Śmigielski, M.; Stuart, F.M.; Persano, C.; Sinclair, H.D. Structure and evolution of the Carpathian thrust front between Tarnów and Pilzno (Pogórska Wola area, southern Poland)—Results of integrated analysis of seismic and borehole data. *Geol. Q.* **2014**, *58*, 399–416. [CrossRef]
35. Górecki, W. (Ed.) *Atlas of Geothermal Waters and Energy Resources in the Western Carpathians*; Ministry of Environment: Kraków, Poland, 2011; pp. 1–412, (In Polish with English Summary).
36. Majorowicz, J.; Polkowski, M.; Grad, M. Thermal properties of the crust and the lithosphere–asthenosphere boundary in the area of Poland from the heat flow variability and seismic data. *Int. J. Earth Sci.* **2019**, *108*, 649–672. [CrossRef]
37. Szafran, S.; Wagner, M. Geotectonic causes of changes in mean reflectance of huminit/vitrinite coalified organic material in Miocene sediments of Carpathian Foredeep. *Zesz. Nauk. Politech. Śląskiej Ser. Górnictwo* **2000**, *246*, 517–532, (In Polish with English Abstract).
38. Kotarba, M.J.; Więcław, D.; Bilkiewicz, E.; Dziadzio, P.; Kowalski, A. Genetic correlation of source rocks and natural gas in the Polish Outer Carpathians and Paleozoic–Mesozoic basement east of Kraków (Southern Poland). *Geol. Q.* **2017**, *61*, 795–824. [CrossRef]
39. Goldbach, M.; Geršlová, E.; Misz-Kennan, M.; Nehyba, S. Thermal maturity of Miocene organic matter from the Carpathian Foredeep in the Czech Republic: 1D and 3D models. *Mar. Petrol. Geol.* **2017**, *88*, 18–29. [CrossRef]
40. Buła, Z.; Habryn, R. Precambrian and Palaeozoic basement of the Carpathian Foredeep and the adjacent Outer Carpathians (SE Poland and western Ukraine). *Ann. Soc. Geol. Pol.* **2011**, *81*, 221–239.
41. Jawor, E.; Baran, U. Geological setting and characteristics of Carboniferous strata in the southern part of the Małopolska block. In *Possibility of Hydrocarbon Generation in Carboniferous Strata in Southern Part of the Małopolska and Upper Silesia Blocks*; Kotarba, M.J., Ed.; Towarzystwo Badania Przemian Środowiska "Geosfera": Kraków, Poland, 2004; pp. 25–48, (In Polish with English Summary).
42. Moryc, W. Geological Structure of Miocene Substratum in Kraków–Pilzno Region. *Nafta-Gaz* **2006**, *6*, 263–282, (In Polish with English Summary).
43. Narkiewicz, M. Development and inversion of Devonian and Carboniferous basins in the eastern part of the Variscan foreland (Poland). *Geol. Q.* **2007**, *51*, 231–256.
44. Maksym, A.; Śmist, P.; Pietrusiak, M.; Staryszak, G.; Liszka, B. New data on development of the Lower Paleozoic sediments in the Sędziszów Małopolski–Rzeszów region based on Hermanowa-1 borehole (SE Poland). *Przegląd Geol.* **2003**, *51*, 412–418, (In Polish with English Summary).
45. Zając, R. Stratigraphy and facies development of the Devonian and Lower Carboniferous in southern part of the Carpathian Foredeep. *Kwart. Geol.* **1984**, *28*, 291–316, (In Polish with English Summary).
46. Dudek, L.; Strzetelski, J.; Botor, D.; Florek, R. Petroleum potential of the Mesozoic-Paleozoic basement in the Bochnia–Tarnów area. *Prace Inst. Górnict. Naft. Gazow.* **2003**, *122*, 1–68, (In Polish with English Summary).
47. Więcław, D.; Kotarba, M.J.; Kowalski, A.; Kosakowski, P. Habitat and hydrocarbon potential of the Palaeozoic source rocks in the Kraków–Rzeszów area (SE Poland). *Ann. Soc. Geol. Pol.* **2011**, *81*, 375–394.
48. Kosakowski, P.; Wróbel, M. Burial and thermal history and hydrocarbon generation modeling of the Lower Palaeozoic source rocks in the Kraków—Rzeszów area (SE Poland). *Ann. Soc. Geol. Pol.* **2011**, *81*, 459–471.
49. Moryc, W. The Permian and Triassic of the Polish Carpathian Foreland. *Biuletyn Państ. Instyt. Geol.* **2014**, *457*, 43–68, (In Polish with English Summary). [CrossRef]
50. Niemczycka, T.; Brochwicz-Lewiński, W. Evolution of the Upper Jurassic sedimentary basin in the Polish Lowland. *Kwart. Geol.* **1988**, *32*, 137–156, (In Polish with English Abstract).
51. Matyja, B.A. Development of the Mid-Polish Trough *versus* Late Jurassic evolution in the Carpathian Foredeep area. *Geol. Q.* **2009**, *53*, 49–62.
52. Kosakowski, P.; Więcław, D.; Kotarba, M.J.; Kowalski, A. Habitat and hydrocarbon potential of the Mesozoic strata in the Kraków–Rzeszów area (SE Poland). *Geol. Q.* **2012**, *56*, 139–152.
53. Kosakowski, P.; Wróbel, M. Burial history, thermal history and hydrocarbon generation modeling of the Jurassic source rocks in the basement of the Polish Carpathian Foredeep and Outer Carpathians (SE Poland). *Geol. Carpath.* **2012**, *63*, 335–342. [CrossRef]

54. Matyasik, I.; Dziadzio, P. Reconstruction of petroleum systems based on integrated geochemical and geological investigations: Selected examples from the middle Outer Carpathians in Poland. In *The Carpathians and Their Foreland: Geology and Hydrocarbon Resources*; Golonka, J., Picha, F.J., Eds.; AAPG Memoir: Washington, DC, USA, 2006; Volume 84, pp. 497–518.
55. Ten Haven, H.L.; Lafargue, E.; Kotarba, M. Oil/oil and oil/source rock correlations in the Carpathian Foredeep and Overthrust, southeast Poland. *Org. Geochem.* **1993**, *20*, 935–959. [CrossRef]
56. Curtis, J.B.; Kotarba, M.J.; Lewan, M.D.; Więcław, D. Oil/source rock correlations in the Polish Flysch Carpathians and Mesozoic basement and organic facies of the Oligocene Menilite Shales: Insights from hydrous pyrolysis experiments. *Org. Geochem.* **2004**, *35*, 1573–1596. [CrossRef]
57. Lewan, M.D.; Kotarba, M.J.; Curtis, J.B.; Więcław, D.; Kosakowski, P. Oil generation kinetics for organic facies with Type-II and -IIS kerogen in the Menilite Shales of the Polish Carpathians. *Geochim. Cosmochim. Acta* **2006**, *70*, 3351–3368. [CrossRef]
58. Kotarba, M.J.; Więcław, D.; Dziadzio, P.; Kowalski, A.; Bilkiewicz, E.; Kosakowski, P. Organic geochemical study of source rocks and natural gas and their genetic correlation in the central part of the Polish Outer Carpathians. *Mar. Petrol. Geol.* **2013**, *45*, 106–120. [CrossRef]
59. Kosakowski, P.; Koltun, Y.; Machowski, G.; Poprawa, P.; Papiernik, B. The geochemical characteristics of the Oligocene—Lower Miocene Menilite formation in the Polish and Ukrainian Outer Carpathians: A review. *J. Petrol. Geol.* **2018**, *41*, 319–335. [CrossRef]
60. Jirman, P.; Geršlová, E.; Pupp, M.; Bubík, M. Geochemical characteristics, thermal maturity and source rock potential of the Oligocene Šitbořice Member of the Menilite Formation in the Ždánice Unit (Czech Republic). *Geol. Q.* **2018**, *62*, 858–872. [CrossRef]
61. Rauball, J.F.; Sachsenhofer, R.F.; Bechtel, A.; Coric, S.; Gratzer, R. The Oligocene–Miocene Menilite Formation in the Ukrainian Carpathians: A world-class source rock. *J. Petrol. Geol.* **2019**, *42*, 141–162. [CrossRef]
62. Wróbel, M.; Kosakowski, P.; Więcław, D. Petroleum processes in the Paleozoic-Mesozoic strata of the Grobla-Limanowa area (basement of the Polish Carpathians). *Geol. Geophys. Environ.* **2016**, *42*, 185–206. [CrossRef]
63. Nemčok, M.; Henk, A. Oil reservoirs in foreland basins charged by thrustbelt source rocks: Insights from numerical stress modeling and geometric balancing in the West Carpathians. *Geol. Soc. Lond. Spec. Pub.* **2006**, *253*, 415–428. [CrossRef]
64. Botor, D. Burial and thermal history of the Upper Silesian Coal Basin (Poland) constrained by maturity modeling—Implications for coalification and natural gas generation. *Ann. Soc. Geol. Pol.* **2020**, *90*, 99–123.
65. Botor, D. Petroleum Systems of the Miocene and Palaeozoic-Mesozoic Substratum in the Carpathians and Carpathians Foredeep (Tarnów—Pilzno Area). Master's Thesis, AGH University of Science and Technology, Faculty of Geology, Geophysics and Environmental Protection, Kraków, Poland, 1994; 56p.
66. Sweeney, J.J.; Burnham, A.K. Evaluation of a simple model of vitrinite reflectance based on chemical kinetics. *AAPG Bull.* **1990**, *74*, 1559–1570.
67. Moryc, W.; Nehring-Lefeld, M. Ordovician between Pilzno and Busko in the Carpathian Foreland (Southern Poland). *Geol. Q.* **1997**, *41*, 139–150.
68. Stefaniuk, M.; Maćkowski, T.; Górecki, W.; Hajto, M.; Zając, A. Distribution modeling of thermal field parameters in the Polish Eastern Carpathians based on geophysical data. In Proceedings of the World Geothermal Congress, Melbourne, Australia, 15–19 April 2015; pp. 108–115.
69. Wygrala, B. Integrated Study of an Oil Field in the Southern Po Basin, Northern Italy. Ph.D. Thesis, University of Cologne, Cologne, Germany, 1989; 226p.
70. Butler, R.W. Hydrocarbon maturation, migration and tectonic loading in the Western Alpine foreland thrust belt. *Geol. Soc. Lond. Spec. Publ.* **1991**, *59*, 227–244. [CrossRef]
71. Mazurek, M.; Hurford, A.J.; Leu, W. Unravelling the multistage burial history of the Swiss Molasse Basin: Integration of apatite fission-track, vitrinite reflectance, and biomarker isomerization analysis. *Basin Res.* **2006**, *18*, 27–50. [CrossRef]
72. Kiersnowski, H. Permo-Triassic sediments in Liplas-Tarnawa Basin. Paleozoic of the basement in the central part of Polish Outer Carpathians (Liplas-Tarnawa zone). *Prace Państw. Inst. Geol.* **2001**, *174*, 85–104, (In Polish with English Abstract).
73. Poprawa, P.; Narkiewicz, K.; Swadowska, E.; Bruszewska, B. Organic maturity and 1-D modeling constraints of hydrocarbon perspectivity in the area Liplas-Tarnawa (Western Carpathians). *Pr. Państw. Inst. Geol.* **2001**, *174*, 173–204, (In Polish with English Abstract).
74. Kowalska, S.; Wójtowicz, A.; Hałas, S.; Wemmer, K.; Mikołajewski, Z.; Buniak, A. Thermal history of Lower Palaeozoic rocks from the East European Platform margin of Poland based on K-Ar age dating and illite-smectite palaeothermometry. *Ann. Soc. Geol. Pol.* **2019**, *89*, 481–509. [CrossRef]
75. Sakaguchi, A. Thermal maturity in the Shimanto accretionary prism, southwest Japan, with the thermal change of the subducting slab: Fluid inclusion and vitrinite reflectance study. *Earth Planet. Sci. Lett.* **1999**, *173*, 61–74. [CrossRef]
76. Świerczewska, A. The interplay of thermal and structural histories of the Magura Nappe (Outer Carpathians) in Poland and Slovakia. *Mineral. Pol.* **2005**, *36*, 91–144.
77. Carr, A.D.; Uguna, C.N. Some thoughts on the influence of pressure and thermal history assumptions on petroleum systems modeling. *J. Petrol. Geol.* **2015**, *38*, 459–465. [CrossRef]
78. Sachsenhofer, R.F. Syn- and post-collisional heat flow in the Cenozoic Eastern Alps. *Int. J. Earth Sci.* **2001**, *90*, 579–592. [CrossRef]
79. Schegg, R.; Leu, W.; Cornford, C.; Allen, P.A. New coalification profiles in the Molasse Basin of western Switzerland: Implications for the thermal and geodynamic evolution of the Alpine foreland. *Eclog. Geol. Helvet.* **1997**, *90*, 79–96.
80. Hurai, V.; Marko, F.; Tokarski, A.; Świerczewska, A.; Kotulova, J.; Biroň, A. Fluid inclusion evidence for deep burial of the Tertiary accretionary wedge of the Carpathians. *Terra Nova* **2006**, *18*, 440–446. [CrossRef]

81. Andreucci, B.; Castelluccio, A.; Jankowski, L.; Mazzoli, S.; Szaniawski, R.; Zattin, M. Burial and exhumation history of the Polish Outer Carpathians: Discrimiating the role of thrusting and post-thrusting extension. *Tectonophysics* **2013**, *608*, 866–883. [CrossRef]
82. Castelluccio, A.; Mazzoli, S.; Andreucci, B.; Jankowski, L.; Szaniawski, R.; Zattin, M. Building and exhumation of the Western Carpathians: New constraints from sequentially restored, balanced cross sections integrated with low-temperature thermochronometry. *Tectonics* **2016**, *35*, 2698–2733. [CrossRef]
83. Sowiżdżał, K.; Słoczyński, T.; Matyasik, I.; Stadtmüller, M. Analysis of Paleozoic petroleum system in the marginal zone of the Carpathian flysch overlap. *Nafta-Gaz* **2015**, *71*, 632–646, (In Polish with English Abstract).
84. Mikulski, S.Z.; Williams, I.S.; Markowiak, M. Carboniferous–Permian magmatism and Mo-Cu (W) mineralization in the contact zone between the Małopolska and Upper Silesia blocks (South Poland): An echo of the Baltica–Gondwana collision. *Int. J. Earth Sci.* **2019**, *108*, 1467–1492. [CrossRef]
85. Filipiak, P.; Jurczak-Drabek, A.; Karwasiecka, M.; Krieger, W. Organic matter in the clastic and coal-bearing Carboniferous deposits of Jachówka-2K, Sułkowice-1, Wysoka-3 and Zawoja-1 boreholes. *Przegląd Geol.* **2002**, *50*, 752–761.
86. Kotarba, M.J.; Kosakowski, P.; Burzewski, W. Hydrocarbon generation and expulsion processes based on 1-D modeling and generation potential of Carboniferous strata in the southern part of the Upper Silesian and Małopolska blocks under Carpathians overthrust. In *Hydrocarbon Generation Potential of Carboniferous Rocks in the Southern Part. of the Upper Silesian and Małopolska Blocks*; Kotarba, M.J., Ed.; TBPŚ "Geosfera": Kraków, Poland, 2004; pp. 87–116, (In Polish with English Summary).
87. Geršlová, E.; Goldbach, M.; Geršl, M.; Skupien, P. Heat flow evolution, subsidence and erosion in Upper Silesian Coal Basin, Czech Republic. *Int. J. Coal Geol.* **2016**, *154–155*, 30–42. [CrossRef]
88. Koltun, Y.; Espitalié, J.; Kotarba, M.; Roure, F.; Ellouz, N.; Kosakowski, P. Petroleum generation in the Ukrainian External Carpathians and the adjacent foreland. *J. Petrol. Geol.* **1998**, *21*, 265–288. [CrossRef]
89. Karnkowski, P. *Oil and Gas. Fields in Poland. Vol. II Oil and Gas. Fields in the Carpathians and Carpathian Foredeep*; Towarzystwo Geosynoptyków "Geos" AGH: Krakow, Poland, 1993; (In Polish with English Abstract).
90. Sowiżdzał, K.; Słoczyński, T.; Sowiżdzał, A.; Papiernik, B.; Machowski, G. Miocene biogas generation system in the Carpathian Foredeep (SE Poland): A basin modeling study to assess the potential of unconventional mudstone reservoirs. *Energies* **2020**, *13*, 1838. [CrossRef]
91. Gaupp, R.; Matter, A.; Platt, J.; Ramseyer, K.; Walzebuck, J. Diagenesis and fluid evolution of deeply buried Permian (Rotliegende) gas reservoirs, NW Germany. *AAPG Bull.* **1993**, *77*, 1111–1128.
92. Picha, F.; Peters, K.E. Biomarker oil-to-source rock correlation in the Western Carpathians and their foreland, Czech Republic. *Petrol. Geosci.* **1998**, *4*, 289–302. [CrossRef]
93. Moldowan, J.M.; Frederick, J.F.; Carlson, R.M.K.; Young, D.C.; Duvne, G.; Clardy, J.; Schoell, M.; Pillinger, C.T.; Watt, D.S. Rearranged hopanes in sediments and petroleum. *Geochim. Cosmochim. Acta* **1991**, *55*, 3333–3353. [CrossRef]
94. Ekweozor, C.M.; Udo, O.T. The oleananes: Origin, maturation and limits of occurrence in southern Nigeria sedimentary basins. *Org. Geochem.* **1988**, *13*, 131–140. [CrossRef]
95. Hunt, J.M. *Petroleum Geochemistry and Geology*, 2nd ed.; W.H. Freeman and Company: New York, NY, USA, 1996.
96. Więcław, D. Origin of liquid hydrocarbons accumulated in the Miocene strata of the Polish Carpathian Foredeep and its Palaeozoic–Mesozoic basement. *Ann. Soc. Geol. Pol.* **2011**, *81*, 443–458.
97. Kowalska, S.; Wolański, K.; Botor, D.; Dunkl, I.; Wójtowicz, A.; Jonkis, U.; Buniak, A. Complex thermal history reconstruction of Carboniferous rocks from the Fore-Sudetic Monocline—Application in a tight gas exploration of illite K-Ar and zircon helium dating. In Proceedings of the EuroClay Conference, Edinburgh, UK, 5–10 July 2015; p. 428.
98. Botor, D.; Papiernik, B.; Maćkowski, T.; Reicher, B.; Kosakowski, P.; Machowski, G.; Górecki, W. Gas generation in Carboniferous source rocks of the Variscan foreland basin: Implications for a charge history of Rotliegend deposits with natural gases. *Ann. Soc. Geol. Pol.* **2013**, *83*, 353–383.
99. Radkovets, N.Y.; Kotarba, M.J.; Koltun, Y.V.; Kowalski, A.; Kosakowski, P.; Więcław, D. Origin and migration of oil from the Ukrainian Outer Carpathians to their Mesozoic basement: The case of the Lopushna traps. *Geol. Q.* **2016**, *60*, 133–148. [CrossRef]